PHILOSOPHICAL TRANSACTIONS A

rsta.royalsocietypublishing.org

Research

Cite this article: Woodhouse J, Putelat T, McKay A. 2015 Are there reliable constitutive laws for dynamic friction? *Phil. Trans. R. Soc. A* **373**: 20140401.
http://dx.doi.org/10.1098/rsta.2014.0401

Accepted: 19 March 2015

One contribution of 11 to a theme issue 'A field guide to nonlinearity in structural dynamics'.

Subject Areas:
materials science, mechanics, wave motion

Keywords:
friction, stick–slip, rate-and-state, brake squeal, violin

Author for correspondence:
Jim Woodhouse
e-mail: jw12@cam.ac.uk

THE ROYAL SOCIETY PUBLISHING

Are there reliable constitutive laws for dynamic friction?

Jim Woodhouse[1], Thibaut Putelat[2] and Andrew McKay[1]

[1]Department of Engineering, University of Cambridge, Trumpington Street, Cambridge CB2 1PZ, UK
[2]Department of Engineering Mathematics, University of Bristol, Queen's Building, University Walk, Bristol BS8 1TR, UK

Structural vibration controlled by interfacial friction is widespread, ranging from friction dampers in gas turbines to the motion of violin strings. To predict, control or prevent such vibration, a constitutive description of frictional interactions is inevitably required. A variety of friction models are discussed to assess their scope and validity, in the light of constraints provided by different experimental observations. Three contrasting case studies are used to illustrate how predicted behaviour can be extremely sensitive to the choice of frictional constitutive model, and to explore possible experimental paths to discriminate between and calibrate dynamic friction models over the full parameter range needed for real applications.

1. Introduction

In many areas of physical science, the underlying governing equations for behaviour are regarded as quite securely known, and most academic and applied research is devoted to solving those equations in one way or another. However, there are still subjects that have a more nineteenth century feel to them: the scientific method of hypothesis, experiment, refutation and refinement is still actively in use to determine suitable governing equations. A prime example of this comes in the general area of constitutive modelling of materials: for example, although many fluids are approximately Newtonian, there are also many possibilities for non-Newtonian behaviour. Other examples include strain-rate plasticity theory in solid mechanics [1–3], and

the wide area of mechanical characterization of biological tissues [4]. The topic of interest in this article is another such area, the characterization of the time-dependent friction force at a sliding interface.

Structural vibration driven by interfacial friction, or influenced by it in some significant way, is very widespread: examples range from earthquakes to violin strings, and from vehicle brake squeal to friction dampers in gas turbine fans. In all these cases, there are good reasons to try to model the behaviour so that it can be predicted, controlled or prevented. Any such modelling effort will inevitably require a constitutive description of the frictional interaction, and therein lies the rationale for this paper. Many models for friction have been proposed, each rooted to some extent in experimental measurements, but there is no general understanding of which of these, if any, could be relied upon to give accurate predictions of dynamic response in any given application. That issue will be examined, concentrating on applications relevant to structural vibration; mainly engineering-based problems, but applications in seismology will also be mentioned. When it comes to considering particular models, the emphasis here will be on styles of model accessible to macroscopic measurement techniques, of the general kind normally used in industrial practice, rather than those based on microscopic physics.

The literature relevant to this general subject is vast, and constraints of space force the authors to concentrate on a particular subset. No doubt each reader would have chosen a different subset: the emphasis here simply reflects our personal research focus. We will not discuss friction in biological applications, nor give a detailed survey of the many mathematical studies based on idealized (often non-smooth) models of friction. We will not review the full range of studies on the nano/microscale origins of friction, whether atomistic [5,6] or asperity-scale [7], nor the blossoming research topics of spatio-temporal frictional slip onset and patterning [8–14]. Further information can be found in substantial reviews [15,16], but also in [17,18] for the more historical aspects of friction research, in [19,20] for the acoustics of friction and in [21] for computational statistical mechanics of low-velocity friction.

The wide range of application problems in which friction is important to vibration can be organized into categories based on the physical details of the process, and also on the questions of most interest. It will be argued that problems in different categories may require friction models with differing degrees of complexity and fidelity: models developed and validated in one context cannot necessarily be expected to perform adequately in another context, even when the contacting materials are the same. Correspondingly, the experimental methods needed to discriminate between and calibrate dynamic friction models will also differ between applications. Examples from three different application areas will be shown in §3.

(a) Frictional damping

The first class of problems covers those in which the main effect of friction is to provide damping. If vibration of a structure causes relative sliding at one or more interfaces, this results in energy dissipation. In some cases, frictional damping is deliberately introduced and very carefully designed, as in the frictional dampers between the blades of turbine fans [22]. More commonly, frictional damping is a side effect of constructional details, as occurs with bolted or riveted joints in many built-up structures like bridges or ships. The overall damping level of most such built-up structures is dominated by effects occurring at joints, sometimes called ‘system damping’ or ‘boundary damping’ [23,24]. It is usually hard to predict the damping level with any accuracy, and it can be a significant source of variability of dynamic response between nominally identical structures, such as vehicles from a production line.

(b) Stick–slip and position control

A related class of problems is typified by the control of robotic manipulators. Stick–slip friction at joints can make it hard to achieve smooth motion or to maintain good positioning accuracy. A major engineering interest is then focused on the design of control strategies to avoid the effect or to cope with it [20].

(c) Self-excited vibration: stability thresholds

However, neither of these effects of friction at joints is the main focus of this paper. Instead, attention is directed to problems where the frictional interaction is a direct cause of vibration, rather than simply modifying the details of pre-existing motion. Examples of friction-driven vibration involve a wide range of length scale and time scale: from geological faults to the atomic force microscope, from years to microseconds. Problems also differ as to which aspects of behaviour are of most interest, and that gives rise to further sub-categories.

For many applications, brake squeal being an example, the main task of the engineer is to try to prevent friction-excited vibration from occurring. A vehicle brake obviously involves a deliberate sliding interface, and the most important goal of squeal modelling is to predict the conditions under which the state of steady sliding is and is not stable. Once any kind of instability occurs, some kind of undesirable noise and vibration is likely to ensue. Understanding the details of this fully developed motion may not be particularly helpful: the aim is to avoid the initiation. An earthquake event is also an instability of a kind [25], but in this case, it is hardly feasible to prevent slippage occurring at geological faults. However, it would be very valuable to understand the instability condition enough to predict the occurrence of violent slips, for example by monitoring precursor signals. The variable of most interest in this case is the stress drop during the slip event, which governs the energy release during the earthquake [26].

Many examples of brake squeal show self-excited vibration that grows progressively from small beginnings, so that a linearized approach to the stability calculation may be relevant. The same is true of some other applications where friction-excited vibration is unwanted. The literature of these subjects is dominated by such linearized studies, in which complex eigenvalues of the governing equations are sought, then the conditions investigated under which at least one eigenvalue migrates to the unstable half of the complex plane. Other problems, such as earthquakes and the bowed violin string, appear to show a different kind of initiating instability. From an initial state of sticking (or slow creep), a sudden gross slip occurs. The motion that follows may be relatively brief, as in the case of an earthquake, or sustained in a periodic or non-periodic way, as in the violin string. It is not obvious whether linearized analysis is useful for such problems: motion appears to be strongly nonlinear from its outset, or at least from very soon afterwards. But bifurcation analysis of one kind or another may still shed light on possible regimes of motion.

(d) Self-excited vibration: limit cycle prediction

In some applications, most obviously the violin string, vibration is intended to occur. The interesting questions for analysis are not to do with whether the string vibrates or not, but centre around the range and details of different periodic regimes of oscillation, and the transitions between these regimes. These give the final two categories of problem. Investigating the detailed form of periodic limit cycles is the simpler of the two problems, and it is one that has been widely studied in many different contexts. For the violin problem, the waveform of periodic motion relates directly to questions of tone quality, and what the instrument maker or the musician can do to vary that tone quality. In more conventional engineering applications, the form of the periodic motion may be important because it determines the frequency content of the excitation signal. This in turn will determine the pattern of noise and vibration propagated to remote parts of a structure, where it may cause noise nuisance, fatigue problems and so on.

(e) Self-excited vibration: transient prediction

The final, and most challenging, category of problem arises when the analyst wishes to produce reliable predictions of the details of transient responses. This can refer to the temporal details of transients, for example at the start of a note on the violin: musical perception of sounds is strongly influenced by transient details, and violinists spend a lot of time practicing to control them (e.g.

[27]). In the context of seismology, 'transients' would include the nucleation phase of a major slip. But in a wider range of problems, 'transients' could also relate more broadly to the pattern of regions of parameter space where the different regimes can be found, and the nature of transitions between regimes when a boundary is crossed. For a wide-ranging discussion of such issues in the wider context of nonlinear dynamical systems, see [28].

2. Types of friction model

There are two distinct stages of building a model of friction. The first involves asking what variables the friction force (i.e. shear stress at the interface) is likely to depend on: in other words, which state variables should enter the governing equation. The second stage is to ask what the mathematical form of those equations should be. This distinction leads to a broader and narrower sense in which the names of models may be used, which causes some confusion in the literature. Two models can involve the same state variable(s) but different functional forms. One might want a name for a class of models involving given variables, or one might want a name associated with a specific form of equation. The distinction will be illustrated in §2c.

There is another important general question about friction models: do they distinguish 'sticking' and 'slipping' as separate states of the system, or not? Some models include the two states, and this tends to lead to mathematically non-smooth problems because of the switching between states. Others have only a single state, and 'sticking' is interpreted as slipping in the form of 'slow creep'. Such models may allow different mathematical techniques to be applied in their analysis [29]. But models of both kinds might be applied to the same problem, and it may not be possible to answer the question 'Is this a smooth or non-smooth problem?' until detailed models have been developed, and their predictions compared with experimental results. For a recent mathematical viewpoint on this connection, see [30,31].

This illustrates a general pitfall. Friction-excited vibration without doubt falls under the general heading of nonlinear dynamics, for which there is a very extensive body of mathematical literature. Within that literature, there are many papers treating problems involving 'friction', but in nearly all cases these papers start with a particular assumed governing equation and then proceed to analyse it. There is very little recognition of the uncertainty about the correct governing equation for friction in any particular context, nor is there much consideration of how methods and predictions might change if different models were employed. One particular manifestation of this issue concerns state-space representation. Much of the theoretical literature of nonlinear dynamics is set in a suitable state space. So the first question a mathematician may ask about a problem is 'what is the state space?' But until a decision has been made about how many state variables are needed in the friction model, this question obviously cannot be answered.

(a) 'Dry' versus 'lubricated' friction

The literature relating to frictional 'laws' has two broad strands, which can be labelled as 'dry friction' and 'lubricated friction', depending on whether there is a friction-modifying layer between the solid surfaces at the interface. This layer can be deliberate, like oil or violin rosin, or accidental, like rain or fallen leaves between a railway wheel and the rail, or in the case of the melt lubrication of ice skates it is the result of local melting at the surface of the ice. Similar local melting can happen when a geological fault slips (e.g. [32]). Although the boundary between the two strands of literature is rather blurred, in practice the two have developed largely independently. However, it will be argued here that the current state of understanding exhibits some strong parallels between the two.

The inclusion of violin rosin as a 'lubricant' may seem a little odd. Rosin, also known as 'colophony', is the solid residue from certain natural tree resins after the more volatile components have been separated by heating. It consists mainly of various resin acids, especially abietic acid. Rosin is used in many contexts as a friction enhancer: not only for coating the hairs of violin bows, but also for example to help gymnasts and dancers keep a good grip on things.

The layer of rosin on a violin bow makes stick–slip friction occur very readily, but, as will be seen in §3c, the mechanism by which it does this is closely related to the behaviour of lubricating oil in a rolling mill or between gear teeth.

(b) Rough surfaces, Coulomb's laws and contact stiffness

The literature of dry friction emphasizes the central role of surface roughness, meaning that all interfacial forces are confined to the tips of interacting asperities. An individual pair of asperities in contact can be expected to deform more or less in accordance with Hertzian contact theory (e.g. [33]), and statistical analysis of many random asperities then leads to a prediction that the real area of contact will be proportional to the applied normal load [34]. This is believed to be the physical basis for the well-known Amontons–Coulomb 'law' that the net friction force during sliding is independent of the apparent area of contact of the two bodies, and proportional to the normal load [35]. The notion of a 'coefficient of friction' μ relies on this proportionality: the friction force τ can then be written as

$$\tau = \mu N, \tag{2.1}$$

where N is the normal load. It will be shown later that in some situations this proportionality is emphatically not satisfied, so the theoretical underpinning will need to be revisited.

There is another important effect of the interacting asperities: they can exhibit a small amount of elastic deformation, in both the normal and the tangential directions, in response to the mean stresses in those directions. This results in normal and tangential contact stiffnesses of the interface, so that even during true sticking at the asperity tips there may be some relative motion between the two bodies when measured remotely from the contact. Whether this contact stiffness is included in a model of 'friction' is largely a semantic question, but some of the friction models from the literature do include it. For asperities, it makes some sense to include contact stiffness in a 'friction' model, as any remote measurement of the shear traction and displacement across an interface will include the effect. The case is less obvious for something like a rubber tyre, where the elastic deformation is big enough to see and measure, so that it might be taken into account as a separate entity (e.g. [36]).

The third ingredient of what elementary textbooks often call 'Coulomb's laws' states that the coefficient of friction is independent of sliding speed. The only variation allowed within this familiar model is that the maximum value of sticking friction, the 'static coefficient of friction', may be larger than the 'dynamic coefficient' during sliding (e.g. [37]).

(c) The friction-curve model

By far the most common measurement of sliding frictional behaviour is of the mean frictional force between surfaces forced to slide at a given steady rate. Such measurements usually reveal that the third Coulomb 'law' is not well satisfied, even approximately: the coefficient of friction is found to be a function of relative sliding speed. A brake manufacturer, having done a 'full tribological characterization' of a brake lining material by mapping out how the coefficient of friction for steady sliding varies with sliding speed under different ambient conditions, may well assume that they can then use these data directly to predict squeal based on a very widely used family of models for friction: the friction force is assumed to depend on a single state variable, the instantaneous relative sliding speed across the interface. We will use the term 'friction-curve model' to describe this generic class of models. The literature also contains terms such as the 'Stribeck model', which usually refer to particular assumed functional forms of the variation with speed.

While it is easy to understand why such a model might be proposed on the basis of a plot of tribometer measurements against sliding speed, this class of models gives a first example of the issue raised earlier, that different models are needed when asking different questions. Brake squeal can occur across the entire audible frequency range, up to tens of kilohertz. There is no logical reason to suppose that at such frequencies the dynamic friction force will simply track

back and forth along the curve deduced from steady sliding at a range of different speeds. As will be shown in §3b, when dynamic measurements are made, they indeed show quite different behaviour. Steady-sliding measurements, and the friction-curve model, do not describe the mechanics of the sliding interface well enough to address even the simplest question about brake squeal: under what circumstances will a braking system show a linearized instability?

(d) Other measurements, other state variables

The only other measurement routinely carried out in the context of industrial applications of friction involves forced reciprocating sliding between two surfaces. Such measurements are used in the characterization of friction dampers [22], and the results are usually interpreted in terms of a model that combines a friction-curve model with the effects of tangential contact stiffness. A well-known example is the so-called LuGre model [38]. Models of this type bring in an additional state variable in the form of the displacement of the contact spring and are often used in the analysis of problems of the kind discussed in §1a,b. They are particularly useful in contexts where it is necessary to take account of the finite size of the contact region, to allow for the possibility of sticking in part of the region while slipping in the remainder, as is responsible for 'fretting wear' for example [33].

In a wider context, a number of other styles of friction measurement have been used. A brief summary will be given here, and some of them are then taken up in more detail in §3. A classical experiment involves a block on an inclined plane: the maximum slope that permits sticking to continue gives directly the static coefficient of friction, while the smallest slope that allows sliding to continue once started gives the dynamic coefficient. Rabinowicz [39] extended this experiment by applying calibrated impulses to the block and documented an intermediate range where the block would start to slide but then stop. He argued that the results were consistent with a model involving a 'critical slip distance', beyond which the static coefficient of friction reduces to the dynamic value.

Another set of experiments also involves a block that can slide, but now restrained by a spring. The spring is pulled, or equivalently the surface beneath the block is made to move, and the conditions are investigated under which steady sliding is seen, as opposed to regular or irregular slip–stick motion. The transition between the regimes gives evidence about the underlying friction law [40,41]. One version of this experiment is known as the surface force apparatus (e.g. [5,42]), in which the contacting surfaces are covered with atomically smooth cleaved mica, and then a controlled amount of the material to be tested is introduced to the contact: in other words, the experiment concentrates on lubricated friction. On the other hand, similar experiments on dry friction have been performed (e.g. [43]).

In both cases, the results have been argued to be consistent with a family of friction models known as the 'rate and state models'. These models were first motivated, though, by a different experiment. Dieterich was interested in seismic applications, and performed tests using rock samples [44]. In the earliest of these experiments, polished rock surfaces were forced to slide against each other, and then the sliding speed was abruptly changed. Before the friction force settled to the new value corresponding to the new steady speed, a transient response was observed. Typically, the initial change in friction force had the opposite sign to the eventual change determined by the steady friction curve. The measurements immediately suggested that some other internal state variable must be involved, with a time evolution responsible for the observed transient. The resulting model will be discussed in §2e.

But before that it is useful to finish this summary of measurement methods that shed light on dynamic friction. There are two more types of measurement relevant to this article. The first could be thought of as an extension of the Dieterich measurement, in that it involves modulation of the speed of sliding. As mentioned at the end of §2c, the friction-curve model has been shown to be inadequate to address the question of the threshold of stability for linearized friction-driven vibration. But it is easy to see what information *is* needed for a linearized study. If sliding speed is perturbed by a low-amplitude sinusoid of given frequency, then under any circumstances for

which linear theory is applicable, the resulting perturbation to the friction force must also be sinusoidal, at the same frequency. The amplitude and phase of the force perturbation, relative to the velocity perturbation, may vary with frequency. This amplitude and phase relation is the information required about the friction law for this type of application: it is a kind of frequency response function [45]. Some measurements of this frequency response will be shown in §3b.

The final type of measurement to be mentioned involves deliberately inducing stick–slip motion in a system with known dynamical behaviour, and inferring the time-varying friction force by some kind of inverse calculation. The earliest example was by Ko & Brockley [43], who used a system similar to the spring–mass system mentioned above. Newton's law for the motion of the mass allows the friction force to be calculated from measured motion once the mass, stiffness and damping constant are known. They used these measurements to demonstrate the inadequacy of the friction-curve model for their particular system and materials. A somewhat similar experiment by Smith & Woodhouse [46] used a cantilever-like oscillator driven into stick–slip vibration by a rosin-coated rod to provide evidence for the required friction model for rosin. A related experiment by Schumacher and co-workers used a vibrating string rather than a cantilever, 'bowed' by a rosin-coated glass rod. Velocity and force at the contact point were deduced by inverse calculation based on measured forces at the string's terminations. The bowed-string problem will be discussed further in §3c, where it will be argued that the most important state variable in the friction law for violin rosin is the temperature in the contact zone.

(e) Rate-and-state models

In the most general sense, any friction model is a 'rate-and-state' model: the friction force is determined by the current values of the normal load N and the relative sliding speed v, plus one or more additional state variables required to represent whatever other physics is necessary. These additional variables, which will have their own evolution equations, may have direct physical interpretations such as local temperature or some measure of the condition of the contacting asperities. Alternatively, some of them may be introduced for mathematical convenience, as when it is required to express a higher order differential equation as a set of first-order equations for a state-space formulation. A further distinction is that a state variable like contact temperature has its evolution governed by a partial differential equation, bringing in spatial complexity, whereas it is often assumed that the relevant state variables are governed by simpler evolution equations.

A widely studied family of models of this latter type takes the form

$$\tau = F(N, v, \psi) \tag{2.2}$$

with

$$\dot{\psi} = -G(N, v, \psi), \tag{2.3}$$

where ψ is the state variable, or vector of state variables. Two functions F and G are introduced, and some specific proposed functions will be seen shortly. Following [47], a negative sign is introduced in equation (2.3) to indicate that the expected behaviour is a relaxation process. In most of the existing literature, Coulomb's law is assumed, so that the dependence on N is trivial and the equations can be written directly in terms of the coefficient of friction μ without mention of N.

It is important to distinguish between the instantaneous value of the friction force and the value that would be found under steady sliding with the same speed. For a constant value $v = V$, this is obtained by first solving

$$G(N, V, \psi_{ss}) = 0 \tag{2.4}$$

for the steady-state value of the state variable(s) ψ_{ss} and then evaluating

$$\tau_{ss} = F(N, V, \psi_{ss}). \tag{2.5}$$

A concise but comprehensive introduction to classical rate-and-state friction models arising from rock mechanics and seismology can be found in Rice *et al.* [47]. So far, these models have been

largely phenomenological in nature, different realizations of equations (2.2) and (2.3) having been proposed in order to fit experimental datasets (e.g. [48]). Historical realizations of such models of friction share the same expression for the friction coefficient:

$$\mu = \frac{\tau}{N} = \mu_* + a \ln\left(\frac{v}{V_*}\right) + b \ln\left(\frac{\psi}{\psi_*}\right) \tag{2.6}$$

while the state evolution laws are different:

$$\dot{\psi} = 1 - \frac{v\psi}{L} \quad \text{(Dieterich ageing law [49])} \tag{2.7}$$

or

$$\dot{\psi} = -\left(\frac{v\psi}{L}\right) \ln\left(\frac{v\psi}{L}\right) \quad \text{(Ruina slip law [49])}. \tag{2.8}$$

In these models, the key parameter that controls the state relaxation process is a memory length L, related to the critical slip distance of Rabinowicz [39,50,51]. The subscript $_*$ denotes characteristic reference values.

These equations were first formulated in a context where the slip velocity was always positive, but for the wider class of applications, it is necessary to allow negative speeds and this renders the logarithmic terms problematic. The friction force is expected to satisfy a simple symmetry condition: reversing the sliding direction reverses the friction force. This motivates a modified version of the classical equations (2.6)–(2.8), when combined with the fact that the expression (2.6) can be physically motivated (e.g. [47,52] and references therein) either:

(i) by the 'Bowden–Tabor product decomposition' of the interfacial shear stress, based on considerations of interfacial asperity deformation, which suggests that

$$\tau \equiv A_{\mathrm{r}}(\psi)\tau_{\mathrm{c}}(v), \tag{2.9}$$

where A_{r} refers to the real interfacial contact area and τ_{c} is an asperity yield or creep stress measure associated with deformation mechanisms determined by a thermally activated rate process; or

(ii) by assuming that the probability of asperity slip events is also governed by a thermally activated rate process associated with an Arrhenius law. Arguments based on microscale creep deformation mechanisms then lead to predictions for the form of the rate-and-state coefficients a and b [47,52]. A regularized form has thus been proposed for the generic family of rate-state friction models:

$$\mu = a \sinh^{-1}\left[\frac{1}{2}\frac{v}{V_*} \exp\left(\frac{E(\psi)}{k_{\mathrm{B}}T}\right)\right], \tag{2.10}$$

where the state-dependent energy of activation may be defined as

$$E(\psi) = k_{\mathrm{B}}T \frac{\mu_* + b \ln(c + \psi/\psi_*)}{a}, \tag{2.11}$$

so as to follow the Dieterich–Ruina models in the limit of large argument for the $\sinh^{-1}$ function; k_{B} and T denote the Boltzmann constant and the absolute temperature. In (2.11), a small residual strength parameter c has also been inserted to introduce a velocity-strengthening regime for relatively high speeds [41,53], but below the flash temperature critical velocity [54].

A specific example of this family has been studied most extensively [41], and will be used in the computations to be shown in §3. This takes the form (2.10) with (2.11), with

$$\psi_* = \frac{L}{L + V_* t_{**}} \tag{2.12}$$

Table 1. Material parameter values for 'Bristol board' from [40], used in the rate-and-state simulation studies here.

material	μ_*	a	b	L [m]	V_* [m s^{-1}]	c	$R = t_{**}V_*/L$
paper	0.369	0.0349	0.0489	0.9×10^{-6}	10^{-6}	10^{-3}	100

in association with the state evolution law

$$\dot{\psi} = \frac{1-\psi}{t_{**}} - \frac{|v|\psi}{L}. \tag{2.13}$$

Note that the two additional parameters t_{**} and c make steady friction non-monotonic, referred to as 'spinodal' friction. For the case $b > a$, there is a local maximum and minimum of the friction coefficient located at $v_M \approx (L/t_{**})/(b/a-1)$ and $v_m \approx (b/a-1)V_*/c$, respectively. Alternative expressions of spinodal friction models can be devised [41] following the Bowden–Tabor product decomposition (i) or by introducing some elastic interfacial compliance [12,55]. Furthermore, a set of parameter values have been fitted to measurements by Baumberger and co-workers [40,56] on the friction behaviour of a paper product known as Bristol board. These values are listed in table 1. An excellent review, including the physical underpinnings of the friction model, has been given by Baumberger & Caroli [57]. Applications and experimental foundation of such models in the context of earthquake mechanics are thoroughly discussed in [49,58].

Whether governing equations of this form give satisfactory predictions for a given friction-driven vibration problem now becomes a question for experimental exploration. It has already been suggested in various literature that this model family can match experimental results for a range of tests. Indeed, a degree of convergence has been shown: similar equations, with different physical internal state variables. For example, the Rabinowicz and LuGre models can be cast into this mathematical form. However, although this model works well in several different contexts, it should be noted that the data to support this assertion were mostly obtained at very slow sliding speeds and relatively long time scales.

This has two consequences. First, it means that dynamic thermal effects may not be very significant because changes are slow enough for the local temperature to remain close to equilibrium ambient conditions. Second, it means that the validation of the fitted friction law is confined to long time scales, or equivalently to low frequencies. Some authors have explicitly acknowledged this limitation (e.g. Baumberger & Caroli [57]). For applications in the field of structural vibration, high sliding speeds and frequencies up into the kilohertz range are of concern, so further exploration is needed. This issue is taken up in §3: it will be shown later that when measurements have been made at higher frequencies, the results suggest that an enhanced friction model is needed.

3. Case studies

(a) Rate-and-state friction and the mass–spring–slider model

The simplest relevant model system is a single degree of freedom oscillator excited by friction, so it is not surprising that this is a widely studied problem. It can be visualized as a mass m restrained by a linear spring of stiffness k, pressed with a normal force N against a belt moving at speed V, with the desired frictional law acting between the mass and the belt. For the simplest case of Coulomb friction with a dynamic coefficient of friction that is independent of sliding speed (or any other state variable), this problem can be solved in closed form by elementary methods (e.g. [35,37]). Sustained stick–slip motion is possible provided that $\mu_s > \mu_d$. With more complicated friction laws, even this simple system generally requires numerical simulation to obtain response time histories. The system makes a good test-bed to explore the influence of different friction models on the detailed form of the vibration response, and thus give clues about possible experimental strategies for probing frictional constitutive laws. Some results

will be shown in this subsection, based on the family of rate-and-state laws introduced in the previous section.

One aspect of the behaviour that is amenable to analytic calculation is the stability condition for the state of steady sliding. The result can be written in several different ways. For the general model given by (2.2)–(2.5) with a single-state variable ψ, one way to state the condition is in terms of a critical spring stiffness: the steady-state solution $v = V$ becomes unstable through a Hopf bifurcation when [40,41,48,59,60]

$$k \le k_0 + m\omega_c^2 \tag{3.1}$$

where the quasi-static critical stiffness k_0 and angular frequency ω_c are given by

$$k_0 = -\frac{\partial G}{\partial \psi}\frac{\mathrm{d}\tau_{ss}}{\mathrm{d}v} \quad \text{and} \quad \omega_c^2 = -\left(\frac{\partial G}{\partial \psi}\right)^2 \frac{\mathrm{d}\tau_{ss}}{\mathrm{d}v} \Big/ \frac{\partial \tau}{\partial v}. \tag{3.2}$$

This result fits in with a familiar result for friction-curve models: steady sliding of an undamped oscillator like this is linearly unstable for a velocity-weakening friction law [48,60], as is physically obvious since the linearized friction law represents a 'negative damper'. That result is extended here to velocity-weakening behaviour of the steady-state friction force τ_{ss}. For the classical Dieterich/Ruina models (2.6)–(2.8), the specific result has

$$k_0 = \frac{(b-a)N}{L} \quad \text{and} \quad \omega_c = \sqrt{\frac{b}{a} - 1}\left(\frac{V}{L}\right). \tag{3.3}$$

The instability condition can also be written in terms of angular frequency:

$$\omega^2 \le \omega_0^2 + \omega_c^2, \quad \text{where } \omega = \sqrt{\frac{k}{m}} \quad \text{and} \quad \omega_0 = \sqrt{\frac{k_0}{m}}. \tag{3.4}$$

Alternatively, in terms of the normal force the condition reads, assuming (2.1),

$$N \ge -k \Big/ \left(\frac{\partial G}{\partial \psi}\frac{\mathrm{d}\mu_{ss}}{\mathrm{d}v}\right) - m\frac{\partial G}{\partial \psi} \Big/ \frac{\partial \mu}{\partial v} := N_c(V). \tag{3.5}$$

This last version is useful from an experimental perspective, because in a practical experiment it may be easy to vary the normal force, but much less easy to change the stiffness or natural frequency of the oscillator.

It is now interesting to explore the question of what kind of measurements could be done with a test rig approximating this simple mass–spring–slider system, to find out whether a friction-curve model or a rate-and-state model within a particular family gives an adequate description of the self-excited vibration. To that end, systematic simulations can be performed covering a chosen region of parameter space, and the results assessed using a variety of metrics. Examples of the pattern of variation of these metrics across the parameter space can be presented graphically, to reveal whether any given metric gives sensitive discrimination between friction models. Conversely, if no metric can be found that discriminates between certain models, that would give evidence that it might not matter very much which of those models was chosen.

The specific model studied is based on the spinodal law of equations (2.10)–(2.13), using the parameter values for Bristol board listed in table 1. A two-parameter family of cases has been explored, for convenience of graphical presentation. One parameter is the normal force N, to be regarded as something that could easily be varied in an experiment. The second parameter is chosen to create variations in the friction law. A scale factor λ is introduced to the evolution law for the single assumed state variable so that it formally becomes $\lambda\dot{\psi} = -G(v, \psi)$.

As $\lambda \to 0$, the evolution of the state variable becomes so fast that it will simply track the steady-state value ψ_{ss}. The result is that the friction force obeys a friction-curve model based on μ_{ss}. As λ increases, the timescale of state-variable evolution gets longer so that the interaction of the friction law with the time scale of the oscillation can be explored. However, the steady-sliding relation $\mu_{ss}(v)$ is unchanged by the value of λ. This is important because one might expect to calibrate any experimental rig by measuring $\mu_{ss}(v)$ before performing dynamic tests with self-excited vibration.

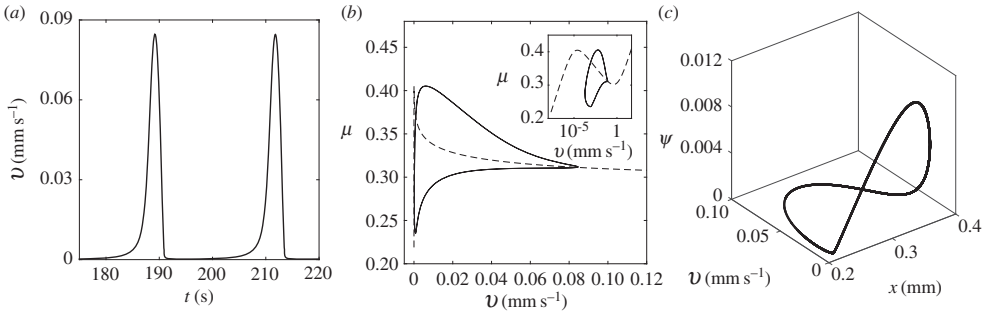

Figure 1. Simulation of stick–slip motion for a mass–spring driven by a spinodal law (2.10)–(2.13) for $m = 1$ kg, $k = 1.09$ N m^{-1}, $V = 10^{-2}$ mm s^{-1}, $\lambda = 10$ and N/mg $= 10^{-4}$: (*a*) slip velocity waveform; (*b*) trajectory in the μ–v plane for the spinodal law (solid line) and the steady sliding relation $\mu_{ss}(v)$ (dashed line) with the equivalent μ–log$_{10}(v)$ plot inset; (*c*) three-dimensional trajectory.

So the question of interest becomes: for models with a known characteristic $\mu_{ss}(v)$, what should be measured in order to establish (i) whether any model of the tested family is consistent with the results, (ii) whether the value of λ makes a significant difference to the motion, and (iii) how to establish the correct value of λ.

An example of a simulated periodic motion is shown in figure 1. The parameter values are listed in table 1. Figure 1*a* shows the sliding speed: it is clear that the motion shows a 'stick–slip' cycle, except that the relative sliding speed v never falls quite to zero during the 'sticking' episodes because of the particular friction law chosen. Figure 1*b* shows the trajectory in the μ–v plane, and it also includes as the dashed line the steady-sliding relation $\mu_{ss}(v)$. It is apparent that the actual trajectory is quite different from the steady-sliding curve in this case. Figure 1*c* shows a three-dimensional phase plot of the motion, with the state variable on the vertical axis. The shape of this curve relates to the obvious asymmetry of the velocity waveform in figure 1*a*. When a sticking episode begins, the state variable has a value near zero and both the velocity waveform and the phase plot show a sharp corner. During sticking, the state variable evolves through significantly non-zero values, and it continues to evolve as slipping recommences, leading to more gentle curves.

Figure 2 shows two versions of the N–λ parameter plane described above. In each case, individual plotted symbols mark the simulation runs used. The vertical scale is logarithmic, but the bottom line of simulations shown in the plots were in fact done with the friction-curve model, in the limit where λ has gone to zero. Where the symbols have a grey plus sign in the centre, the simulation revealed that steady oscillation occurred. The pattern of these symbols matches the prediction of the stability threshold, shown as a solid line. In the top left of the plots, steady sliding was stable and no oscillation occurred. The heavy circle marks the case shown in figure 1: it was chosen to fall near the 'elbow' of the stability threshold where several influences on the detailed motion are active simultaneously.

For cases with oscillation, below the stability line, the plots are colour-shaded according to two examples of metrics that are potentially measurable in a real experiment. Figure 2*a* uses as a metric the proportion of the oscillation period for which sticking was seen. On the left of the diagram, the motion becomes quasi-sinusoidal with only a very short sticking interval, so the value tends towards zero. On the right, by contrast, the motion tends towards that of a 'relaxation oscillator' where sticking predominates, interrupted by very short slipping episodes. The metric thus tends to unity here. The metric used in figure 2*b* is a normalized value of the loop area of the trajectory in the μ–v plane, as shown in figure 1*b*. Over much of the plane, this metric takes very small values, indicating that this aspect of the behaviour, at least, is close to what would be given by the friction-curve model. Only as the stability line is approached do we see significant variation in this metric.

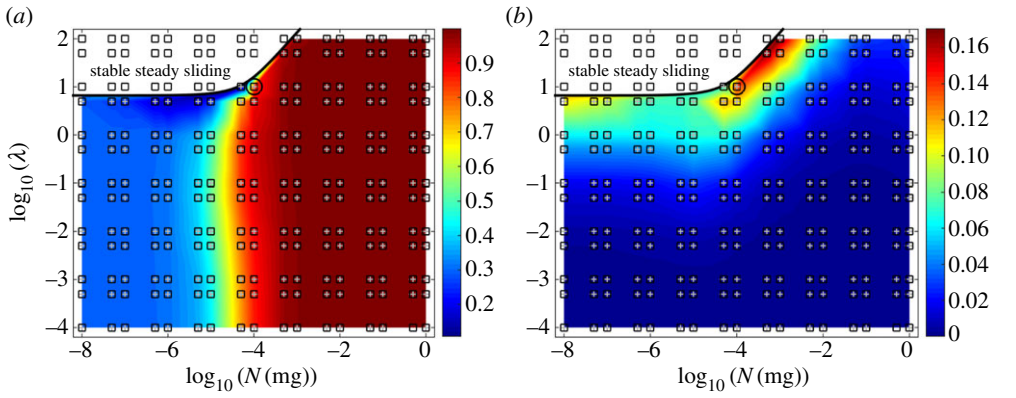

Figure 2. Metrics in the N–λ parameter plane with simulation runs (marked square), runs detected as stick–slip (marked +) and the linearized stability threshold (solid line, see equation (3.5)): (*a*) proportion of oscillation period spent sticking; (*b*) normalized loop area in the μ–v plane. The point marked with a circle corresponds to the case shown in figure 1. (Online version in colour.)

In an experiment, the normal load N could be varied but the friction model, parametrized by λ, is a given. One could thus imagine probing the behaviour along horizontal lines in the parameter plane. Of the two sample metrics shown here, the first gives little opportunity to detect the influence of different values of λ, because the colours show vertical stripes indicating insensitivity to the friction model. The second metric is more promising, as it shows interesting variation along vertical lines, at least near the top of the region plotted. Examining such plots with a variety of metrics could allow experimental studies to be designed to give some hope for discriminating between friction models of this kind.

Finally, it can be mentioned that the weakly nonlinear study of such oscillators may provide experimentalists with additional useful constraints for the identification of rate-and-state friction models, from tracking the possible behaviour change of the stick–slip Hopf bifurcation as reported in [41,56]. Deeper inside the stick–slip domain, when the full nonlinear regime is attained, it is also possible that the location of further bifurcations of periodic orbits and the cartography of the transitions between regimes may also give useful discriminating information. Along those lines, it should be noted that period-doubling bifurcation cascades have been reported for systems similar to the one studied here (e.g. [61,62]). However, from a practical point of view, measurements of friction are generally rather noisy, and it is far from clear whether complicated transitions, including chaos, could be reliably detected. The sources of erratic dynamics in frictional systems are numerous (e.g. [63–65]) and can obscure the contribution of interfacial friction. Nevertheless, there has been at least one attempt at empirical identification of friction models using chaotic dynamics [66]; see [15] for additional references. In any case, in engineering applications, it would be rare that prediction of chaotic regimes was the main objective of modelling.

(b) Linearized analysis of squeal instabilities

The second case study in dynamic friction concerns a different aspect of frictional behaviour. As explained earlier, if the purpose of characterizing friction of a sliding interface is in order to perform linearized stability predictions for phenomena like brake squeal, then a very different style of measurement is called for from that suggested in §3a. If linear theory is to be valid, then a small sinusoidal perturbation imposed on a steady sliding speed must evoke a sinusoidal variation in friction force (and perhaps in normal force as well). The relative amplitude and phase of the force variation relative to the velocity perturbation may vary with frequency, to

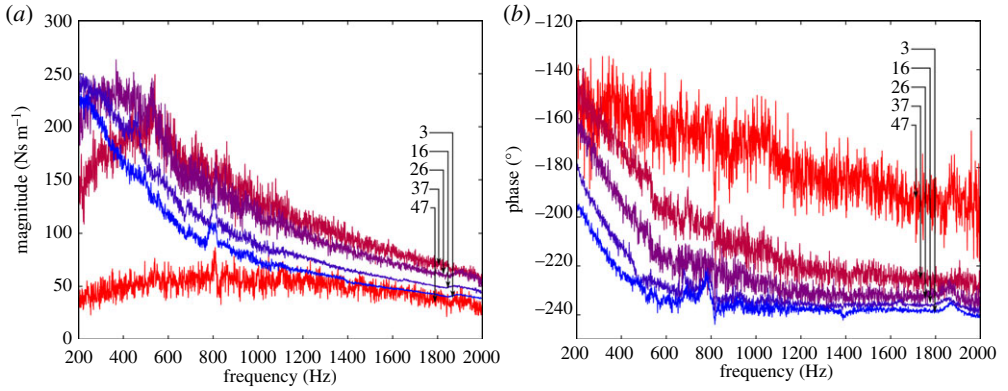

Figure 3. Transfer functions relating the small perturbation in friction force to an imposed small perturbation of sliding speed, for a nylon pin in contact with a glass disc, in (*a*) amplitude and (*b*) phase. The steady sliding speed was 2 mm s^{-1} in all cases, and normal loads were 3, 16, 26, 37 and 47 N for the separate plots, with colours grading from blue (3 N) to red (47 N). Adapted from [45]. (Online version in colour.)

form a kind of frequency response function of sliding friction. For this particular aspect of friction dynamics, it is convenient to move away from the time-domain viewpoint and adopt a frequency-domain view.

Some preliminary measurements of this frequency response function for a sliding frictional contact have been made [45,67]. The test rig, described in detail in [45], is of the pin-on-disc variety: a small pin of one chosen material is loaded against a disc of a second material, which can be driven in steady rotation. The pin is carried on a mechanism that can be actuated in the sliding direction to impose controlled fluctuations of sliding speed. By driving this actuator with band-limited random noise, standard methods of vibration measurement can be used to obtain an averaged transfer function, with the associated coherence function to give an indication of whether linear theory is valid (e.g. [20,68]). An advantage of this test method is that moderately high frequencies can be explored: published measurements [45,67] to date extend up to 2 kHz.

One example of the results is shown in figure 3, for measurements using a nylon pin in contact with a glass disc. Curves are shown for five different values of the normal force, all at the same sliding speed. Encouragingly, good coherence was observed, and also the results were shown to be independent of excitation amplitude (provided it was sufficiently small). It appears that, at least for this material combination, it is indeed possible to find a meaningful linearized friction description.

Two things are immediately clear from figure 3. First, the frequency response certainly is a complex function of frequency. If the friction-curve model had been relevant to this test, a constant, real value would have been obtained: the slope of the friction curve at the chosen mean sliding speed. Such a model can thus be immediately ruled out for these materials and sliding conditions. Second, the normal force has a non-trivial influence on the results: both amplitude and phase plots show different shapes with different normal loads, whereas if Coulomb's law had been applicable, the amplitude curves would have scaled in proportion to N, while the phase curve would be unchanging.

This second observation is somewhat puzzling because the mean value of the friction force, measured simultaneously with the dynamic tests, did follow Coulomb's law quite accurately [45, fig. 9]. This suggests that, although the nominal contact area in this experiment is quite small, the usual description in terms of a statistical distribution of random asperity contacts would seem to hold, so that the friction force is proportional to the real area of contact, which is in turn proportional to normal load. But the dynamic component of friction force, shown in figure 3, reveals a more complicated dependence on normal load. The conclusion must be either that the

dynamic force component is not simply proportional to the real area of contact, or that normal load is having an influence on the friction force by an additional route.

To address this question and to explain the pattern of frequency variation revealed by the measurement obviously require comparisons with theoretical models. It is easy enough to take any particular theoretical model and linearize it to produce a prediction to compare with the measurements. Some comparisons of this kind have been made [67], but none of the published studies show satisfactory agreement. The classical rate-and-state models predict a form of frequency variation that is similar in some respects to the measurements, but wrong in detail. A simple model involving local temperature as a state variable has also been explored [67]. This introduces an influence of the normal load via the rate of heating, which is separate from an effect of the real area of contact, but it does not appear to show the right pattern of behaviour to give even qualitative agreement with the measured results.

A similar procedure could be applied to any other friction model, although no others have yet been published. It is possible that the observations may prove to be consistent with a model already available in the literature. The most promising candidate models, based on recent work, combine rate-and-state friction models with the effect of tangential contact stiffness, along the lines of [12,55]. Such models are showing some promise, and it seems likely that a resolution of this puzzle will be forthcoming before long. If the usual Coulomb law is assumed for the actual friction force, such a model naturally introduces an influence of normal load on the remotely measured combined contact force if, for example, the contact stiffness is assumed independent of normal load. In any experimental approach of this kind, there is no way to distinguish between friction as such and other effects such as contact stiffness occurring very close to the contact: a force sensor has to be built in somewhere to measure the interfacial shear force, and anything on the 'live' side of that sensor will be included in the measurement.

In any case, measurements of the kind shown in figure 3 give a new type of experimental probe into frictional constitutive models, allowing data to be collected at much higher frequencies than most previous tests. From the practical perspective of industrial applications aimed at, for example, predicting susceptibility of braking systems to squeal, measurements of this kind give the input data that any linearized squeal theory needs. Tribological characterization of brake lining materials should surely be extended to include measurements of this kind on a routine basis. Without that information, there is very little hope of successful prediction, as has been demonstrated experimentally on a laboratory system which is a simplified version of a disc brake [69,70]. At present, most of the literature relating to brake squeal uses very primitive frictional models. Most of it, indeed, assumes the basic Coulomb law with a constant coefficient of friction: that case can be treated by a mathematical trick in which the friction effect is incorporated into a non-symmetric stiffness matrix. But the available evidence suggests that this model is likely to be hopelessly unreliable for instability prediction of a multi-modal system like a disc brake. If detailed design studies to mitigate squeal are wanted, it will be necessary to move to better models.

An extension of this 'frequency response' modelling has been proposed. In the prediction of brake squeal, it is important to take account of dynamic interactions in the normal direction as well as the tangential direction, so a full linearized characterization of the contact forces might involve a 2×2 matrix of frequency response functions, rather than just the single function described here [70]. This may link to earlier literature suggesting that normal motion can play a significant role in friction behaviour (e.g. [7,71,72]). However, no measurements of this 2×2 matrix have yet been reported: this a challenge for the future.

(c) The bowed violin string

The final case study concerns the bowed violin string. This is a topic with its own extensive literature, which will not be examined in detail here: for a recent review, see [73]. For the present purpose, two aspects of this literature are important. First, this subject raises particular concerns about the details of transient response, and that makes it especially challenging from

the modelling standpoint. Second, this challenge has been investigated for a long time: the violin string is arguably the most deeply studied of all applications of friction-driven vibration. As a result, it can provide very clear examples of the sensitivity of predictions to the choice of frictional constitutive model, and the difficulty of formulating a model that is sufficiently consistent with experiment to have serious predictive power.

As mentioned earlier, the friction between the bow-hairs and strings of a violin is mediated by a glassy material called rosin. The glass transition temperature is typically only a little above normal room temperature, so that the mechanical properties vary very rapidly with small changes in local temperature. Based on a variety of evidence, it has been argued that temperature is the most important state variable for rosin friction [46]. However, most of the early literature on the violin string, in common with many other friction-driven vibration problems, was based on the friction-curve model in which instantaneous sliding speed was assumed to be the only relevant input variable. A comparison of results will be shown shortly, between the friction-curve model using the measured steady-sliding friction curve and a simple thermal model with the same steady-sliding characteristics.

To motivate the particular comparison to be shown, a little more must be explained about the motion of a bowed string. As was first discovered by Helmholtz [74], violinists are usually trying to achieve a particular periodic motion of the string. This motion, known as the 'Helmholtz motion', involves a single slip in each cycle of stick–slip vibration: see Woodhouse [73] for more details. Violinists have to practice their bowing gestures for a long time to achieve musically satisfactory results, and one of the things they are learning is how to manipulate the bow in order to achieve initial transients that settle into Helmholtz motion quickly [27].

A particular two-parameter family of bowing gestures was studied by Guettler, with a view to understanding how players achieve such transients [75]. This family of gestures involves the bow starting in contact with the string, with a certain normal force. The bow is then accelerated from rest with constant acceleration. The values of normal force and acceleration form the two parameters of this family. Guettler argued that there is a wedge-shaped region of this space within which 'perfect' starting transients might be achievable. A measured version of this 'Guettler diagram' is shown in figure 4*a*. The open D string of a cello has been bowed, using a computer-controlled bowing machine, in a 20×20 grid of gestures covering a region of the parameter plane. The string motion was captured using a sensor embedded in the bridge to measure the transverse force exerted by the vibrating string. An example transient is shown in figure 5: the sawtooth waveform after about 0.1 s is the signature of Helmholtz motion. The 400 waveforms were analysed by computer to classify the length of the transient before Helmholtz motion was established, and this transient length is coded in the colour scale of figure 4*a*.

The results show a trace of Guettler's predicted wedge-shaped region, but the data are 'speckly': the transient length varies from pixel to pixel, and even within the wedge there are some black pixels that did not produce Helmholtz motion at all but a different regime of nonlinear oscillation. In fact, the experiment gives a hint of sensitive dependence: even with the computer-controlled bowing machine, repeating the parameter space scan does not produce identical results but a different pattern of speckles.

However, the underlying wedge-shaped region within which Helmholtz motion is produced, at least sometimes, persists. The task of theoretical modelling is to produce a set of simulations capable of reproducing this behaviour with sufficient fidelity that the model might be trusted to shed light on how the details of the pattern might be affected by changes to the string, or the instrument body behaviour, or some other musically relevant aspect. Modelling of the linear part of the system is reasonably uncontroversial [73], and the main challenge comes, as elsewhere in this paper, from the friction model. Figure 4*b* shows the result of simulations using the friction-curve model based on measured steady-sliding properties of rosin. It is immediately obvious that this model gives very poor results: hardly any aspects of the pattern are successfully reproduced. Among other things, the model results are even more speckly than the measurements. Whether this model, or indeed the real physical system, shows chaos in the formal mathematical sense is not known, but on the basis of these plots it would not be surprising. Bowed-string models have

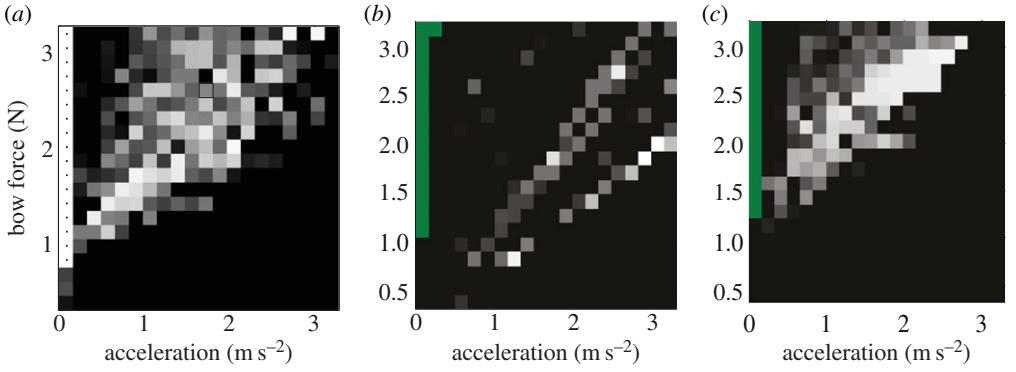

Figure 4. Guettler diagrams (see text) for the open D string of a cello: (*a*) measured; (*b*) simulated using a friction-curve model; (*c*) simulated using a thermal friction model sharing the same steady-sliding characteristic with case (*b*). Grey scale encodes transient length, from zero (white) to 20 period-lengths or greater (black). From the perspective of a musician, white pixels show 'perfect starts' to a note. Outlined square in (*a*) marks the transient shown in figure 5. (*a*) Adapted from [76] and (*b*, *c*) from [77]. (Online version in colour.)

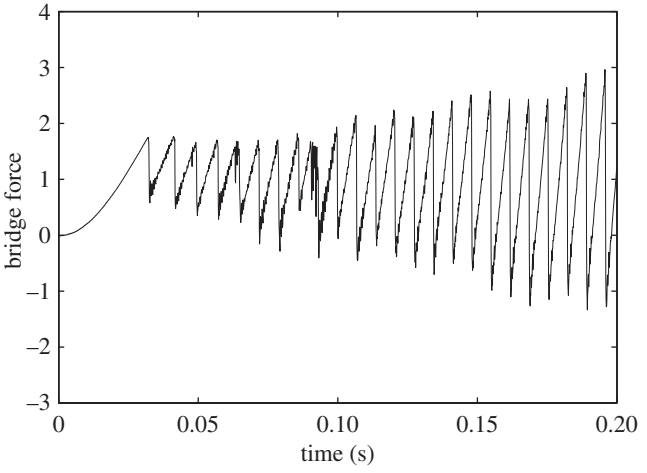

Figure 5. Example bowed-string transient with a constant normal bow force, and bow motion accelerating from rest with constant acceleration, with parameter values corresponding to the outlined square in figure 4*a*. The plotted waveform shows transverse force exerted by the vibrating string at the bridge of the cello, the input force that drives body vibration. The sawtooth waveform towards the right-hand side is 'Helmholtz motion' (see text). Adapted from [76].

far too many degrees of freedom to allow the application of the usual mathematical techniques of dynamical systems theory.

Figure 4*c* shows corresponding simulations using a friction model in which the state of sliding is envisaged as plastic yielding with a yield stress that is a function of local contact temperature. A heat flow model is run alongside the dynamic simulation in order to give predictions of the time-varying contact temperature: the governing equation is, of course, more complicated than the simple first-order evolution equation assumed in the rate-and-state models such as equations (2.6)–(2.8). The yield stress as a function of temperature is fixed by requiring that the model reproduces the steady-sliding friction law as measured, and also as used in the friction-curve simulations of figure 4*b*. The results show a closer match, at least qualitatively, to the measurements of figure 4*a*, but the agreement is far from perfect and examination of individual transients reveals details that are not well captured by the simulations. These results clearly show the sensitive influence of the assumed friction model on the predictions. Further, they hint at the

difficulty of achieving a model that is good enough to have predictive power in this particular application problem. The simple thermally driven model gives encouraging results, but certainly not good enough, and the challenge to produce a better model remains.

Ideally, one would like a model that uses the bulk properties of rosin, measured or modelled, in a convincing simulation of what happens within the contact region between bow and string. Some progress has been made in that direction. A natural starting point is given by work on elasto-hydrodynamic lubrication, which has led to a model for the shear behaviour of materials of this general kind based on the Eyring model: the shear strain rate $\dot{\gamma}$ is related to the (absolute) temperature T, the pressure P and the shear stress τ by the relation

$$\dot{\gamma} = \frac{\dot{\tau}}{S} + KT \exp\left(-\frac{E_a + PV_a}{k_B T}\right) \sinh\left(\frac{\tau}{\tau_*}\right), \tag{3.6}$$

where S is the elastic shear modulus, and the other quantities are material constants specific to the lubricant [78–81]. A generic similarity can be noted with the model suggested in the previous case study, combining rate-and-state friction with a contact stiffness. The term involving the shear modulus here gives an effect corresponding to the tangential contact stiffness. The result is an interesting convergence between 'dry' and 'lubricated' friction models.

From this viewpoint, violin rosin behaves in a mirror-image fashion to a lubricant film in a rolling mill, for example. This constitutive equation combines aspects of solid and fluid behaviour. Note that increasing pressure makes the behaviour more solid, whereas increasing temperature makes it more liquid. In a rolling mill, the lubricant film enters the nip of the rollers in a liquid state, and although there is local heating due to slip, the pressure effect wins over the temperature effect and the film behaves in a solid-like way in the nip. Violin rosin on the bow hair at room temperature is a solid, but in the contact region with the string, although the pressure can be very high, the high slip rates mean that the temperature effect wins over the pressure effect, and the rosin behaves like a liquid.

The bow–string contact can be simulated on the basis of this model, and this reveals some interesting behaviour. Within the layer of rosin, typically a few micrometres thick, the thermally softening nature of rosin as the glass transition is approached means that as shear motion in the layer commences, it tends to become localized into a shear band perhaps of the order of 100 nm thick. Temperatures within this very thin active layer may fluctuate over a range of the order of 30°C in every cycle of the string's vibration. However, further work is needed to develop a fully satisfactory model of the process, because the Eyring model taken at face value makes some predictions that are not borne out by experiment. The reason appears to be closely parallel to remarks made earlier about the rate-and-state models of dry friction: the measurements on which the Eyring law is based were carried out with rather long time scales, and it seems likely that in an application like the violin string involving much shorter time scales, additional details of the underlying physics will need to be taken into account. This possibility was anticipated by Tabor, who wrote [81] 'There is some evidence that the phase change is relatively sluggish. Thus [the Eyring model] must be applied with some caution since the lubricant film is in the contact region for a very short time'.

4. Conclusion

In an overwhelming proportion of the literature of friction-excited vibration, authors begin by assuming a friction 'law' without any attempt at detailed justification of whether it is appropriate or reliable for the particular problem in hand. In this article, it has been suggested that such an approach is often doomed to failure. Several proposed friction laws from the literature of physics, mechanics and seismology have been reviewed. Three contrasting case studies have been used to demonstrate that (i) different assumed friction laws can make a big difference to the predicted behaviour, and some familiar assumptions (such as the simple Coulomb model) may be so crude that one might question whether they *ever* give reliable predictions for details of friction-excited vibration, (ii) friction laws that are well validated in one kind of application, or by

one kind of measurement, cannot be relied upon to work well in different settings (although of course if the model embodies a correct description of the underlying physics, it is more likely to work when extended to a new domain), and (iii) different levels of sophistication in the required output from a prediction require correspondingly different levels of sophistication in the friction model.

Furthermore, it has been pointed out that nearly all published experimental work on dynamic friction is limited to very low frequencies and/or very slow sliding speeds. Two examples of experimental work at higher frequencies, into the kilohertz range required by many engineering vibration applications, have been presented that show the appearance of new phenomena. In the case of interfacial frictional characterization suitable for use in the prediction of linearized thresholds for brake squeal, for example, the measurements so far published have proved not to be consistent with some popular models of dynamic friction, and further extension of these models is clearly required. In the case of the bowed violin string, with a stringent requirement to predict transient details of the string's motion correctly, things are even more complicated. There is evidence that local temperature in the contact region plays a key role in determining the friction force, but a fully satisfactory model agreeing with measurements has yet to be formulated and validated.

There is a need for these issues to be appreciated more clearly by any researcher hoping to predict friction-driven vibration. There is also a need to develop more sophisticated measurement methods to allow models to be tested and calibrated over the full parameter range needed for real applications. Some useful techniques have been developed, but few of them have yet been taken up by end users such as manufacturers of automotive braking systems. In short, the constitutive laws underlying dynamic friction still offer a wide range of research challenges for theoreticians and experimentalists alike, and many opportunities for debate between pure and applied scientific communities.

Data accessibility. The Matlab script used to generate figures 1 and 2, and the experimental data used for figures 3–5 are available on request: contact the corresponding author.

Authors' contributions. All three authors contributed to the general overview in §§1 and 2, and helped draft the manuscript. T.P. provided the theoretical discussion in §§2e and 3a. A.M. carried out the numerical work in figures 1 and 2. J.W. provided the experimental data used in figures 3–5.

Competing interests. We declare we have no competing interests.

Funding. A.M. and T.P., respectively, acknowledge support from the CUED EPSRC Doctoral Training award and the EPSRC programme grant 'Engineering Nonlinearity' (ref. EP/K003836/1).

Acknowledgements. The authors thank Tore Butlin, Alessandro Cabboi, Alan Champneys and Robert Szalai for helpful and stimulating discussions, and also two anonymous reviewers for valuable comments.

References

1. Fleck NA, Willis JR. 2009 A mathematical basis for strain-gradient plasticity theory. Scalar plastic multiplier. *J. Mech. Phys. Solids* **57**, 161–177. (doi:10.1016/j.jmps.2008.09.010)
2. Fleck NA, Willis JR. 2009 A mathematical basis for strain-gradient plasticity theory. Tensorial plastic multiplier. *J. Mech. Phys. Solids* **57**, 1045–1057. (doi:10.1016/j.jmps.2009.03.007)
3. Fleck NA, Hutchinson JW, Willis JR. 2014 Strain gradient plasticity under non-proportional loading. *Proc. R. Soc. A* **470**, 20140267. (doi:10.1098/rspa.2014.0267)
4. Mofrad MRK, Kamm RD (eds). 2011 *Cytoskeletal mechanics: models and measurements in cell mechanics*. Cambridge Texts in Biomedical Engineering. Cambridge, UK: Cambridge University Press.
5. Bhushan B, Israelachvili JN, Landman U. 1995 Nanotribology: friction, wear and lubrication at the atomic scale. *Nature* **374**, 607–616. (doi:10.1038/374607a0)
6. Gao J, Luedtke WD, Gourdon D, Ruths M, Israelachvili J, Landman U. 2004 Frictional forces and Amontons' law: from the molecular to the macroscopic scale. *J. Phys. Chem. B* **108**, 3410–3425. (doi:10.1021/jp036362l)
7. Dankowicz H. 1999 On the modeling of dynamic friction phenomena. *J. Appl. Math. Mech.* **79**, 399–409. (doi:10.1002/(SICI)1521-4001(199906)79:6<399::AID-ZAMM399>3.0.CO;2-K)

8. Heaton TH. 1990 Evidence for and implications of self-healing pulses of slip in earthquake rupture. *Phys. Earth Planet. Int.* **64**, 1–20. (doi:10.1016/0031-9201(90)90002-F)
9. Rice JR, Ben-Zion Y. 1996 Slip complexity in earthquake fault models. *Proc. Natl Acad. Sci. USA* **93**, 3811–3818. (doi:10.1073/pnas.93.9.3811)
10. Kaneko Y, Avouac JP, Lapusta N. 2010 Towards inferring earthquake patterns from geodetic observations of interseismic coupling. *Nat. Geosci.* **3**, 363–369. (doi:10.1038/ngeo843)
11. Ben-David O, Cohen G, Fineberg J. 2010 The dynamics of the onset of frictional slip. *Science* **330**, 211–214. (doi:10.1126/science.1194777)
12. Bouchbinder E, Brener EA, Barel I, Urbakh M. 2011 Slow cracklike dynamics at the onset of frictional sliding. *Phys. Rev. Lett.* **107**, 235501. (doi:10.1103/PhysRevLett.107.235501)
13. Behrendt J, Weiss C, Hoffmann NP. 2011 A numerical study on stick–slip motion of a brake pad in steady sliding. *J. Sound Vib.* **330**, 636–651. (doi:10.1016/j.jsv.2010.08.030)
14. Di Bartolomeo M, Massi F, Baillet L, Culla A, Fregolent A, Berthier Y. 2012 Wave and rupture propagation at frictional bimaterial sliding interfaces: from local to global dynamics, from stick–slip to continuous sliding. *Tribol. Int.* **52**, 117–131. (doi:10.1016/j.triboint.2012.03.008)
15. Ibrahim RA. 1994 Friction-induced vibration, chatter, squeal, and chaos—Parts I and II. *Appl. Mech. Rev.* **47**, 209–226. (doi:10.1115/1.3111079); 227–253 (doi:10.1115/1.3111080)
16. Berger EJ. 2002 Friction modeling for dynamic system simulation. *Appl. Mech. Rev.* **55**, 535–577. (doi:10.1115/1.1501080)
17. Tabor D. 1981 Friction: the present state of our understanding. *ASME J. Lubr. Technol.* **103**, 169–179. (doi:10.1115/1.3251622)
18. Feeny B, Guran A, Hinrichs N, Popp K. 1995 A historical review on dry friction and stick–slip phenomena. *Appl. Mech. Rev.* **51**, 321–341. (doi:10.1115/1.3099008)
19. Akay A. 2002 Acoustics of friction. *J. Acoust. Soc. Am.* **111**, 1525–1548. (doi:10.1121/1.1456514)
20. Sheng G. 2008 *Friction-induced vibrations and sound: principles and applications*. Boca Raton, FL: CRC Press.
21. Müser MH, Urbakh M, Robbins MO. 2003 Statistical mechanics of static and low-velocity kinetic friction. *Adv. Chem. Phys.* **126**, 187–272. (doi:10.1002/0471428019.ch5)
22. Schwingshackl CW, Petrov EP, Ewins DJ. 2012 Measured and estimated friction interface parameters in a nonlinear dynamic analysis. *Mech. Syst. Signal Process.* **28**, 574–584. (doi:10.1016/j.ymssp.2011.10.005)
23. Nashif AD, Jones DIG, Henderson JP. 1985 *Vibration damping*. New York, NY: Wiley-Interscience.
24. Torvik PJ. 2010 Material and slip damping. In *Harris' shock and vibration handbook*, 6th edn (eds AG Piersol, TL Paez), pp. 35.1–35.29. New York, NY: McGraw-Hill.
25. Bizzarri A. 2014 The mechanics of seismic faulting: recent advances and open issues. *Riv. Nuovo Cimento* **37**, 181–271. (doi:10.1393/ncr/i2014-10099-0)
26. Aki K, Richards PG. 2002 *Quantitative seismology*, 2nd edn. Sausalito, CA: University Science Books.
27. Guettler K, Askenfelt A. 1997 Acceptance limits for the duration of pre-Helmholtz transients in bowed string attacks. *J. Acoust. Soc. Am.* **101**, 2903–2913. (doi:10.1121/1.418520)
28. Thompson JMT, Stewart HB. 2002 *Nonlinear dynamics and chaos*, 2nd edn. New York, NY: John Wiley and Sons.
29. Bernardo M, Budd C, Champneys AR, Kowalczyk P. 2008 *Piecewise-smooth dynamical systems: theory and applications*. Applied Mathematical Sciences, vol. 163. New York, NY: Springer.
30. Jeffrey M. In press. The mathematical description of friction between solid bodies. *Nonlinear Dyn*. (doi:10.1007/s11071-015-2100-7)
31. Szalai R. 2013 Modelling elastic structures with strong nonlinearities with application to stick–slip friction. *Proc. R. Soc. A* **470**, 20130593. (doi:10.1098/rspa.2013.0593)
32. Rice JR. 2006 Heating and weakening of faults during earthquake slip. *J. Geophys. Res. Solid Earth* **111**, B05311. (doi:10.1029/2005JB004006)
33. Johnson KL. 1985 *Contact mechanics*. Cambridge, UK: Cambridge University Press.
34. Greenwood JA, Williamson JBP. 1966 Contact of nominally flat surfaces. *Proc. R. Soc. Lond. A* **295**, 300–319. (doi:10.1098/rspa.1966.0242)
35. Bowden FP, Tabor D. 1950 *The friction and lubrication of solids*. Oxford, UK: Oxford University Press.
36. Pacejka HB. 2005 *Tyre and vehicle dynamics*, 2nd edn. Oxford, UK: Butterworth-Heinemann Ltd.

37. Woodhouse J. 1991 Vibrations: tuning forks and train wheels, squealing brakes and violins. In *New applications of mathematics* (ed. C Bondi), pp. 202–222. London, UK: Penguin.
38. Canudas de Wit CH, Olsson H, Astrom KJ, Lischinsky P. 1995 A new model for control of systems with friction. *IEEE Trans. Autom. Control* **40**, 419–425. (doi:10.1109/9.376053)
39. Rabinowicz E. 1951 The nature of the static and kinetic coefficients of friction. *J. Appl. Phys.* **22**, 1373–1379. (doi:10.1063/1.1699869)
40. Heslot F, Baumberger T, Perrin B, Caroli B, Caroli C. 1994 Creep, stick–slip, and dry-friction dynamics: experiments and a heuristic model. *Phys. Rev. E* **49**, 4973–4988. (doi:10.1103/PhysRevE.49.4973)
41. Putelat T, Dawes JHP, Willis JR. 2010 Regimes of frictional sliding of a spring–block system. *J. Mech. Phys. Solids* **58**, 27–53. (doi:10.1016/j.jmps.2009.09.001)
42. Israelachvili JN. 1991 *Intermolecular and surface forces*. New York, NY: Academic Press.
43. Ko PL, Brockley CA. 1970 The measurement of friction and friction-induced vibration. *J. Tribol.* **92**, 543–549. (doi:10.1115/1.3451468)
44. Dieterich JH. 1979 Modeling rock friction: 1. Experimental results and constitutive equations. *J. Geophys. Res.* **84**, 2161–2168. (doi:10.1029/JB084iB05p02161)
45. Wang SK, Woodhouse J. 2011 The frequency response of dynamic friction: a new view of sliding interfaces. *J. Mech. Phys. Solids* **59**, 1020–1036. (doi:10.1016/j.jmps.2011.02.005)
46. Smith JH, Woodhouse J. 2000 The tribology of rosin. *J. Mech. Phys. Solids* **48**, 1633–1681. (doi:10.1016/S0022-5096(99)00067-8)
47. Rice JR, Lapusta N, Ranjith K. 2001 Rate and state dependent friction and the stability of sliding between elastically deformable solids. *J. Mech. Phys. Solids* **49**, 1865–1898. (doi:10.1016/S0022-5096(01)00042-4)
48. Ruina AL. 1983 Slip instability and state variable friction laws. *J. Geophys. Res.* **88**, 10 359–10 370. (doi:10.1029/JB088iB12p10359)
49. Marone C. 1998 Laboratory-derived friction laws and their application to seismic faulting. *Annu. Rev. Earth Sci.* **26**, 643–696. (doi:10.1146/annurev.earth.26.1.643)
50. Rabinowicz E. 1957 The intrinsic variables affecting the stick–slip process. *Proc. Phys. Soc.* **71**, 668–675. (doi:10.1088/0370-1328/71/4/316)
51. Putelat T, Dawes JHP. 2015 Steady and transient sliding under rate-and-state friction. *J. Mech. Phys. Solids* **78**, 70–93. (doi:10.1016/j.jmps.2015.01.016)
52. Putelat T, Dawes JHP, Willis JR. 2011 On the microphysical foundations of rate-and-state friction. *J. Mech. Phys. Solids* **59**, 1062–1075. (doi:10.1016/j.jmps.2011.02.002)
53. Weeks JD. 1993 Constitutive laws for high-velocity frictional sliding and their influence on stress drop during unstable slip. *J. Geophys. Res. Solid Earth* **98**, 17 637–17 648. (doi:10.1029/93JB00356)
54. Archard JF. 1959 The temperature of rubbing surface. *Wear* **2**, 438–455. (doi:10.1016/0043-1648(59)90159-0)
55. Berthoud P, Baumberger T. 1998 Shear stiffness of a solid–solid multicontact interface. *Proc. R. Soc. Lond. A* **454**, 1615–1634. (doi:10.1098/rspa.1998.0223)
56. Baumberger T, Heslot F, Perrin B. 1994 Crossover from creep to inertial motion in friction dynamics. *Nature* **367**, 544–546. (doi:10.1038/367544a0)
57. Baumberger T, Caroli C. 2006 Solid friction from stick–slip down to pinning and aging. *Adv. Phys.* **55**, 279–348. (doi:10.1080/00018730600732186)
58. Scholz CH. 2002 *The mechanics of earthquakes and faulting*, 2nd edn. Cambridge, UK: Cambridge University Press.
59. Ruina AL. 1980 Friction laws and instabilities: a quasistatic analysis of some dry frictional behavior. PhD thesis, Brown University, Providence, RI, USA.
60. Gu JC, Rice JR, Ruina AL, Tse ST. 1984 Slip motion and stability of a single degree of freedom elastic system with rate and state dependent friction. *J. Mech. Phys. Solids* **32**, 167–196. (doi:10.1016/0022-5096(84)90007-3)
61. Oancea VG, Laursen TA. 1997 Stability analysis of state dependent dynamic frictional sliding. *Int. J. Nonlin. Mech.* **32**, 837–853. (doi:10.1016/S0020-7462(96)00082-0)
62. Erickson B, Birnir B, Lavallée D. 2008 A model for aperiodicity in earthquakes. *Nonlin. Processes Geophys.* **15**, 1–12. (doi:10.5194/npg-15-1-2008)
63. Hoffmann NP. 2007 Linear stability of steady sliding in point contacts with velocity dependent and LuGre type friction. *J. Sound Vib.* **301**, 1023–1034. (doi:10.1016/j.jsv.2006.10.010)

64. Oberst S, Lai JCS. 2011 Chaos in brake squeal noise. *J. Sound Vib.* **330**, 955–975. (doi:10.1016/j.jsv.2010.09.009)
65. Putelat T, Willis JR, Dawes JHP. 2012 Wave-modulated orbits in rate-and-state friction. *Int. J. Nonlin. Mech.* **47**, 258–267. (doi:10.1016/j.ijnonlinmec.2011.05.016)
66. Feeny BF, Moon FC. 2007 Empirical dry-friction modeling in a forced oscillator using chaos. *Nonlin. Dyn.* **47**, 129–141. (doi:10.1007/s11071-006-9065-5)
67. Woodhouse J, Wang SK. 2011 The frequency response of dynamic friction: model comparisons. *J. Mech. Phys. Solids* **59**, 2294–2306. (doi:10.1016/j.jmps.2011.08.006)
68. McConnell KG, Varoto PS. 2008 *Vibration testing: theory and practice*, 2nd edn. Hoboken, NJ: Wiley.
69. Ouyang H, Nack W, Yuan Y, Chen F. 2005 Numerical analysis of automotive disc brake squeal: a review. *Int. J. Veh. Noise Vib.* **1**, 207–231. (doi:10.1504/IJVNV.2005.007524)
70. Butlin T, Woodhouse J. 2011 A systematic experimental study of squeal initiation. *J. Sound Vib.* **330**, 5077–5095. (doi:10.1016/j.jsv.2011.05.018)
71. Tolstoi DM. 1967 Significance of the normal degree of freedom and natural normal vibrations in contact friction. *Wear* **10**, 199–213. (doi:10.1016/0043-1648(67)90004-X)
72. Linker MF, Dieterich JH. 1992 Effects of variable normal stress on rock friction: observations and constitutive equations. *J. Geophys. Res. Solid Earth* **97**, 4923–4940. (doi:10.1029/92JB00017)
73. Woodhouse J. 2014 The acoustics of the violin: a review. *Rep. Prog. Phys.* **77**, 115901. (doi:10.1088/0034-4885/77/11/115901)
74. Helmholtz H. 1912 *On the sensations of tone as a physiological basis for the theory of music*, 4th edn. London, UK: Longmans.
75. Guettler K. 2002 On the creation of the Helmholtz motion in bowed strings. *Acta Acust.* **88**, 970–985.
76. Galluzzo PM, Woodhouse J. 2014 High-performance bowing machine tests of bowed-string transients. *Acta Acust. United With Acust.* **100**, 139–153. (doi:10.3813/AAA.918694)
77. Galluzzo PM. 2003 On the playability of stringed instruments. PhD thesis, University of Cambridge, Cambridge, UK.
78. Tabor D. 1981 The role of surface and intermolecular forces in thin film lubrication. In *Microscopic aspects of adhesion and lubrication* (ed. JM Georges). Tribology Series, vol. 7, pp. 651–682. Amsterdam, The Netherlands: Elsevier.
79. Evans CR, Johnson KL. 1986 The rheological properties of elastohydrodynamic lubricants. *J. Mech. Eng. Sci.* **200**, 303–312. (doi:10.1243/PIME_PROC_1986_200_134_02)
80. Hirst W, Richmond JW. 1988 Traction in elastohydrodynamic contacts. *J. Mech. Eng. Sci.* **202**, 129–144. (doi:10.1243/PIME_PROC_1988_202_098_02)
81. Tabor D. 1991 *Gases, liquids and solids*, p. 309. Cambridge, UK: Cambridge University Press.